Automated classification of bimanual movements in stroke telerehabilitation: a comparison of dimensionality reduction algorithms

PROCEEDINGS OF SPIE

SPIEDigitalLibrary.org/conference-proceedings-of-spie

Automated classification of bimanual movements in stroke telerehabilitation: a comparison of dimensionality reduction algorithms

Barak Ventura, Roni, Surano, Francesco Vincenzo, Porfiri, Maurizio

Roni Barak Ventura, Francesco Vincenzo Surano, Maurizio Porfiri, "Automated classification of bimanual movements in stroke telerehabilitation: a comparison of dimensionality reduction algorithms," Proc. SPIE 11590, Nano-, Bio-, Info-Tech Sensors and Wearable Systems, 1159005 (26 March 2021); doi: 10.1117/12.2581433

SPIE.

Event: SPIE Smart Structures + Nondestructive Evaluation, 2021, Online Only

Automated classification of bimanual movements in stroke telerehabilitation: A comparison of dimensionality reduction algorithms

Roni Barak Ventura[a], Francesco Vincenzo Surano[b], and Maurizio Porfiri[*a,c,d]

[a]Department of Mechanical and Aerospace Engineering, New York University Tandon School of Engineering, 6 MetroTech Center, Brooklyn, NY 11201, USA
[b]Dipartimento di Elettronica e Telecomunicazioni, Politecnico di Torino, Corso Duca degli Abruzzi 24, Torino, 10129, Italy
[c]Department of Biomedical Engineering, New York University Tandon School of Engineering, 6 MetroTech Center, Brooklyn, NY 11201, USA
[d]Center for Urban Science and Progress, New York University Tandon School of Engineering, 370 Jay Street, Brooklyn, NY 11201, USA

ABSTRACT

Stroke survivors commonly experience unilateral muscle weakness, which limits their engagement in daily activities. Bimanual training has been demonstrated to effectively recover coordinated movements among those patients. We developed a low cost telerehabilitation platform dedicated to bimanual exercise, where the patient manipulates a dowel to control a computer program. Data on movement is collected using a Microsoft Kinect sensor and an inertial measurement unit to interface the platform, as well as to assess motor performance remotely. Toward automatic classification of bimanual movements executed by the user, we test the performance of a linear and a nonlinear dimensionality reduction techniques.

Keywords: Data science, dimensionality reduction, motion analysis, rehabilitation

1. INTRODUCTION

Stroke-induced hemiparesis prevents survivors' participation in activities of daily living, adversely impacting their quality of life. Survivors can recover motor function of their paretic limbs by adhering to a rehabilitation regimen, consisting of repetitive, high-intensity exercises.[1] Since they cannot move their paretic limb effectively, survivors undergoing telerehabilitation may move abnormally and, ultimately, reinforce incorrect movements.[2] Holding a rod-shaped instrument with both hands could facilitate appropriate movement of the affected limb along with the preserved limb. Furthermore, bimanual training has been shown to hold clinical value, capitalizing on brain plasticity, neural reorganization, and exercise overflow to recover voluntary motion.[3–5]

In a recent paper,[6] we established an interactive telerehabilitation platform dedicated for bimanual exercise (Figure 1A). The platform consists of a Microsoft Kinect device (Microsoft corporation, Redmond, Washington) and an inertial measurement unit (IMU; MPU-6050, InvenSense Inc., Sunnyvale, California) embedded in a simple wooden dowel (Figure 1B). Patients would stand in front of the Kinect sensor, hold the dowel with both hands, and manipulate it (Figure 1C).

Patients' gestures are translated to actions in a computer program, thereby providing an engaging context to the exercise. Specifically, the patients contribute to a citizen science project by performing standard therapeutic tasks. In principle, patients could select any citizen science project that contributes to a cause. Framing the exercise in an educational and altruistic activity has potential to empower patients, who often experience low self-esteem and self-worth due to their acquired disability.[7,8]

*Further author information: (Send correspondence to M.P.)
M.P.: Email:mporfiri@nyu.edu, Telephone: 1 646 997 3681

Nano-, Bio-, Info-Tech Sensors and Wearable Systems, edited by Jaehwan Kim, Proc. of SPIE Vol. 11590, 1159005 · © 2021 SPIE
CCC code: 0277-786X/21/$21 · doi: 10.1117/12.2581433

In our platform, patients would analyze 360° images of a polluted canal in Brooklyn, New York[9,10] by labeling objects of interest they observe in the image. Patients would begin from a baseline pose, where they hold their arms straight and parallel to the ground. To move the cursor to the left, they would perform horizontal shoulder abduction to the left with both arms, while maintaining the dowel parallel to the ground (Figure 1D). To move the cursor to the right, they would perform horizontal shoulder abduction in the opposite direction, moving both hands to the right side of their body. To move the cursor upward or downward, the patients would flex both shoulders and raise the dowel or extend their shoulders and lower it (Figure 1E). To rotate the image right or left, they would vertically rotate the dowel clockwise or counterclockwise, respectively (Figure 1F). To rotate the image up or down, they would flex or extend their wrists, respectively (Figure 1G). Finally, to select or drop a label, the patients would flex and then extend both elbows, pushing the dowel away from their body (Figure 1H).

Interfacing of the platform was achieved by fusion of sensor data from the Microsoft Kinect and IMU, and application of simple conditional statements. The conditional statements are implemented with respect to the relative position of joints. For example, the cursor would move to the left if the left elbow's position relative to the left shoulder's position along the horizontal axis, parallel to the ground, exceeds a certain threshold, and simultaneously, the right elbow's position relative to the right shoulder's position along the same axis exceeds a different threshold.

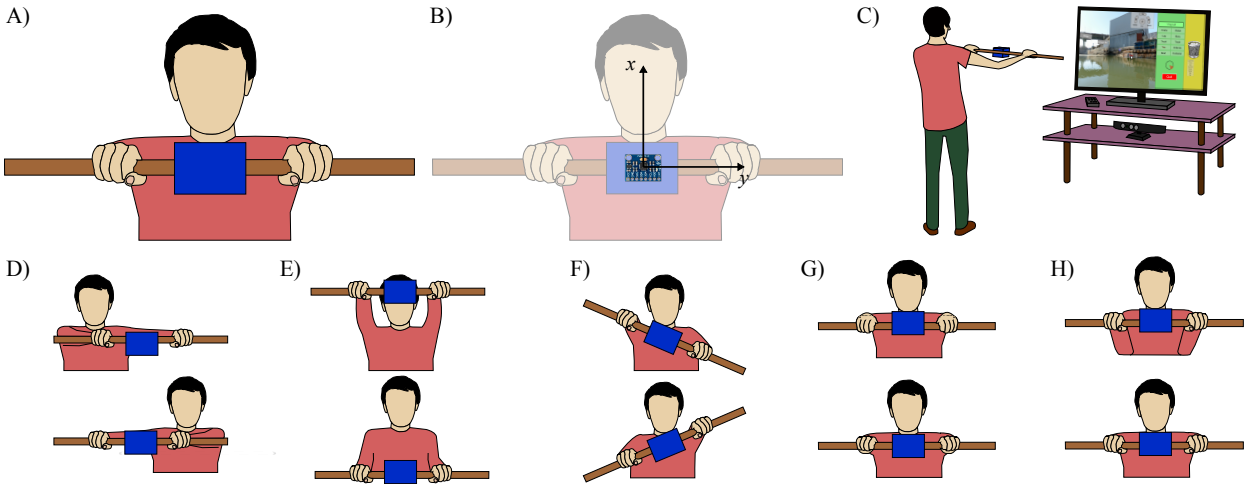

Figure 1. Illustration of the telerehabilitation platform. The user holds a dowel with both hands (A). A 3D-printed box is fixed at the center of the dowel. The box contains an IMU, oriented with its x-axis perpendicular to the dowel and its y-axis parallel to the dowel (z-axis, not shown, is orthogonal to both) (B). The user manipulates the dowel in front of a monitor to perform actions in a citizen science software (C). They can execute five movements to perform in-game actions. In order to move the cursor left or right, the user performs horizontal shoulder abduction (D). In order to move the cursor up or down, the user flexes or extends their shoulders (E). To rotate the image left and right, the user vertically rotates the dowel (F), and to rotate it up and down, the user flexes and extends their wrists (G). To select and drop labels, the user flexes and extends their elbows (H).

To accommodate potential patients' compromised range of motion, the software integrates a calibration phase during which the user performs the aforementioned movements that control the software. They perform each movement and return to the original pose five times, consecutively. The platform records an average of the user's range of motion, and sets the threshold for in-game actions at 20% of it. In this manner, users with a limited range of motion would need to move a smaller distance to induce an action on the screen.

Toward a genuine telerehabilitation paradigm, where users' motor performance is analyzed online and interpretable data is sent to a practitioner for remote assessment, we aim to characterize movements from data collected by the platform. In our earlier work, we pursued a data science approach where we designed features based on a principal component analysis (PCA), and applied a Bagged Trees algorithm to classify movements.[6] Our results demonstrated reliable classification, reaching 93.1% accuracy. In spite of the promising results, our

use of PCA assumes a linear relationship between the variables. Current literature suggests that human motion consists of a linear combination of motor primitives.[11,12] Specifically, muscle flexion and extension are engendered by co-activation of several innervated muscle fibers (also known as synergy[11]), in parallel or in series. However, it is tenable that vision-based recordings of human motion would consist of nonlinear observations. In such a case, alternative methods for dimensionality reductions, such as isomap[13] and diffusion maps,[14] would be more appropriate.

Here, we compare dimensionality reduction of data captured by our platform through PCA and isomap. PCA is a popular method that uncovers manifolds that lie in a linear subspace of the high-dimensionality input space.[15] In its essence, PCA reduces the dimensionality of a data set by identifying fewer orthogonal axes that best preserve the data points' variance.[15] It is easily implemented and considered less computationally intensive than other methods. In contrast, isomap seeks to preserve the geodesic distances between data points.[13] It is particularly useful for recovery of nonlinear manifolds, and represents the global structure of the data set in a single coordinate system. Comparing these methods will provide insight into the nature of human motion data, collected through vision-based sensors.

2. METHODS

2.1 Data collection

Data was collected for a single, healthy subject who moved the dowel along the trajectories predefined in the natural user interface. The first author stood in a baseline pose with her arms held straight and parallel to the ground. She performed the pre-defined bimanual movements as instructed in the calibration, and continued to interact with the software for a short while thereafter.

Two data sets were generated during this exercise. The first data set recorded the subject's joint positions in three dimensions from the Microsoft Kinect sensor. The second data set logged the IMU's Tait-Bryan angles (yaw about the z-axis, α; pitch about the y-axis, β; and roll about the x-axis, γ) and rotational velocities (ω_x, ω_y, and ω_z). Both data sets were collected synchronously at a sampling rate of 18 measurements per second for a duration of 167.9 seconds, generating time series of 3023 time steps.

2.2 Data analysis

The data were processed in MATLAB (MATLAB R2020a, The MathWorks, Inc., Natick, Massachusetts, United States). Only data from the calibration was used, as the sequence of movements the subject performed were known and could be classified. As a first step, a skeleton model of the user's body was reconstructed from the three-dimensional positions of each joint (Figure 2). A reference frame was defined with its origin fixed at the spine, between the shoulder.[16] Its X-axis was parallel to the ground, its Y-axis was perpendicular to ground, and its Z-axis was orthogonal to both, following the right-hand rule. The vectors that corresponded to limb segments were computed by subtraction of the coordinates of the proximal joint from the coordinates of the distal joint.

For each time step, four instantaneous joint angles were computed for each arm: shoulder horizontal abduction ($\theta_{1,\mathrm{R}}$ and $\theta_{1,\mathrm{L}}$), shoulder flexion ($\theta_{2,\mathrm{R}}$ and $\theta_{2,\mathrm{L}}$), wrist flexion ($\theta_{3,\mathrm{R}}$ and $\theta_{3,\mathrm{L}}$), and elbow flexion ($\theta_{4,\mathrm{R}}$ and $\theta_{4,\mathrm{L}}$), where R and L denote the right and left arms, respectively. Horizontal shoulder abduction angles were obtained by projecting the model's upper arm onto the anatomical transverse plane and computing the angle it forms with respect to the anatomical sagittal plane through the inverse tangent. Likewise, shoulder flexion angles were obtained by projecting the model's arm onto the anatomical sagittal plane and computing the angle it forms with respect to the anatomical transverse plane. Elbow and wrist angles were computed using the scalar product between the model's arm and forearm, and between the model's forearm and hand, respectively.

For added insight on the kinematics of movements, instantaneous angular velocities were computed for each joint. A central difference scheme was applied on time series of angle measurements to obtain $\dot{\theta}_{1,\mathrm{R}}$, $\dot{\theta}_{1,\mathrm{L}}$, $\dot{\theta}_{2,\mathrm{R}}$, $\dot{\theta}_{2,\mathrm{L}}$, $\dot{\theta}_{3,\mathrm{R}}$, $\dot{\theta}_{3,\mathrm{L}}$, $\dot{\theta}_{4,\mathrm{R}}$, and $\dot{\theta}_{4,\mathrm{L}}$. Overall, 22 variables were measured at each time step (Table 1).

Time series were visually inspected to identify intervals of movement and the type of movement performed. To standardize the selection of interval boundaries, movement was defined as an instance where IMU rotational

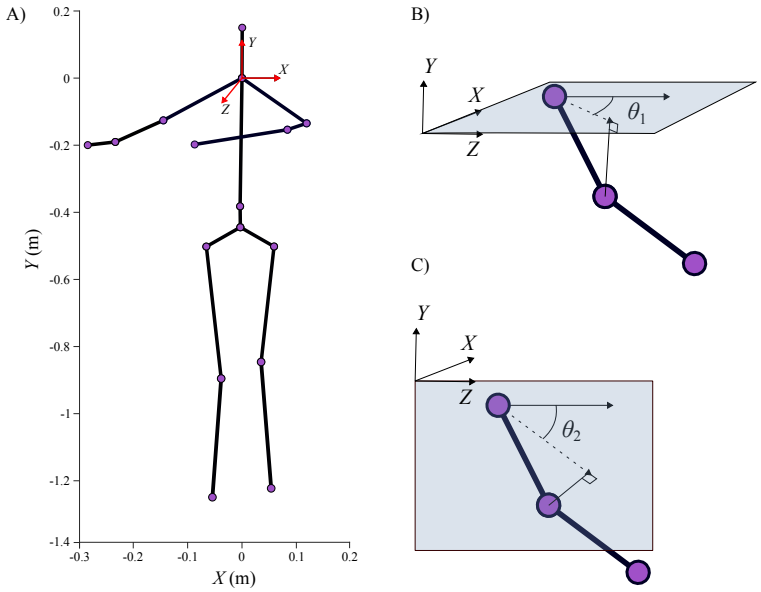

Figure 2. Reconstruction of the user's skeleton from the Microsoft Kinect Data (A). A reference frame is fixed at the model's cervical spine, between the shoulders. The X- and Y-axes are embedded in the anatomical coronal plane, the X- and Z-axes are contained in the transverse plane, and the Y- and Z-axes form the sagittal plane. Horizontal shoulder abduction angle (θ_1) is computed by projection of the model's upper arm onto the anatomical transverse plane (B). Shoulder flexion angle (θ_2) is computed by projection of the model's upper arm onto the anatomical sagittal plane (C).

velocity exceeded 2 deg/s. For each movement type and direction, data points within its intervals were aggregated into a single subset. In total, nine subsets were created: left horizontal shoulder abduction, right horizontal shoulder abduction, shoulder flexion, shoulder extension, counterclockwise rotation, clockwise rotation, wrist flexion, wrist extension, and elbow flexion.

PCA and isomap were applied on the subsets. The isomap algorithm constructed the network based on the Euclidean distances between pairs of data points. For every data point, other data points that were within a fixed radius ϵ were considered as neighbors. The radius was determined as the fifth percentile of all Euclidean distances in the manifold, such that each manifold for each movement had a unique value for ϵ.

3. RESULTS

Both PCA and isomap successfully reduced the dimensionality of each movement type. Embedding of the data set into three dimensions by PCA and isomap yields different manifolds, however, their boundaries are not distinctly demarcated (Figure 3).

For all movements types, residual variances decreased as the dimensionality increased. Nonetheless, residual variances were generally similar between the methods (Figure 4). In all curves, residual variance was slightly lower for isomap than for PCA when reduced to a single dimension. With added dimensions, the effects were soon exchanged and PCA demonstrated lower residual variance than isomap. Points at which the curves abruptly plateau with added dimensions, otherwise known as "elbows", were observed only for shoulder flexion and elbow flexion for both PCA and isomap.

4. DISCUSSION

We present a low-cost platform for bimanual training in stroke telerehabilitation. The platform integrates a simple dowel, an IMU, and a Microsoft Kinect, to create a natural user interface for a dedicated citizen science software. By manipulating the dowel bimanually, patients are able to perform therapeutic movements that are commonly prescribed for home-based rehabilitation, while also contributing to authentic research efforts.

Table 1. Summary of the variables collected by the Microsoft Kinect and IMU. A subscript L or R indicates the left or right arm.

Sensor	Variable	Observation	Notation
Microsoft Kinect	u_1	right shoulder abduction angle	$\theta_{1,\mathrm{R}}$
	u_2	right shoulder flexion angle	$\theta_{2,\mathrm{R}}$
	u_3	right elbow flexion angle	$\theta_{3,\mathrm{R}}$
	u_4	right wrist flexion angle	$\theta_{4,\mathrm{R}}$
	u_5	left shoulder abduction angle	$\theta_{1,\mathrm{L}}$
	u_6	left shoulder flexion angle	$\theta_{2,\mathrm{L}}$
	u_7	left elbow flexion angle	$\theta_{3,\mathrm{L}}$
	u_8	left wrist flexion angle	$\theta_{4,\mathrm{L}}$
	u_9	right shoulder abduction velocity	$\dot{\theta}_{1,\mathrm{R}}$
	u_{10}	right shoulder flexion velocity	$\dot{\theta}_{2,\mathrm{R}}$
	u_{11}	right elbow flexion velocity	$\dot{\theta}_{3,\mathrm{R}}$
	u_{12}	right wrist flexion velocity	$\dot{\theta}_{4,\mathrm{R}}$
	u_{13}	left shoulder abduction velocity	$\dot{\theta}_{1,\mathrm{L}}$
	u_{14}	left shoulder flexion velocity	$\dot{\theta}_{2,\mathrm{L}}$
	u_{15}	left elbow flexion velocity	$\dot{\theta}_{3,\mathrm{L}}$
	u_{16}	left wrist flexion velocity	$\dot{\theta}_{4,\mathrm{L}}$
IMU	u_{17}	roll angle	γ
	u_{18}	pitch angle	β
	u_{19}	yaw angle	α
	u_{20}	rotational velocity about x-axis	ω_x
	u_{21}	rotational velocity about y-axis	ω_y
	u_{22}	rotational velocity about z-axis	ω_z

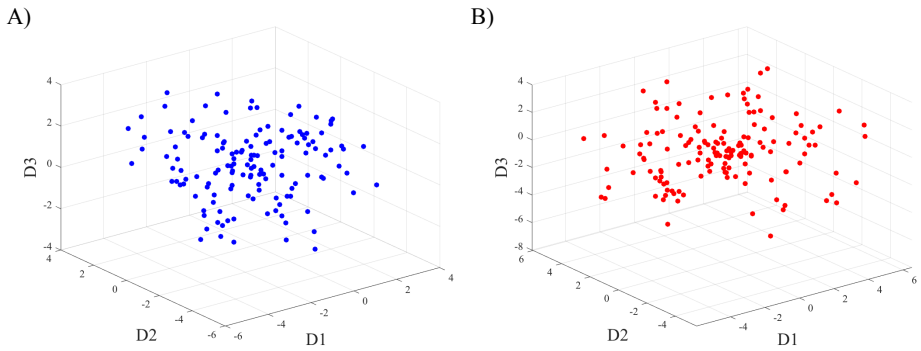

Figure 3. Three-dimensional embedding of the left horizontal shoulder abduction manifold using A) PCA and B) isomap. D1, D2, and D3 represents the first three embedded dimensions. In PCA, these embedded dimensions are principal components, constructed from a linear combination of the original variables. In Isomap, they are nonlinear and need to be inferred by inspection.

Toward consolidation of the platform into a genuine telerehabilitation paradigm, we aim to program classification of movements through data-driven methodologies. Automatic identification of movements would enable real-time feedback to prevent patients from performing undesirable movements,[2] as well as providing clinicians with interpretable scores of motor performance for remote assessment.

To this end, we compared two algorithms for dimensionality reduction: PCA and isomap. If our data was underscored by nonlinear relationships, we would expect isomap to recover a manifold different than the one embedded by PCA. However, isomap created a manifold with no distinct boundaries and visible topology. Furthermore, examination of the residual variance indicated that both methods equally preserve variation. Therefore, it seems that isomap does not outperform PCA.

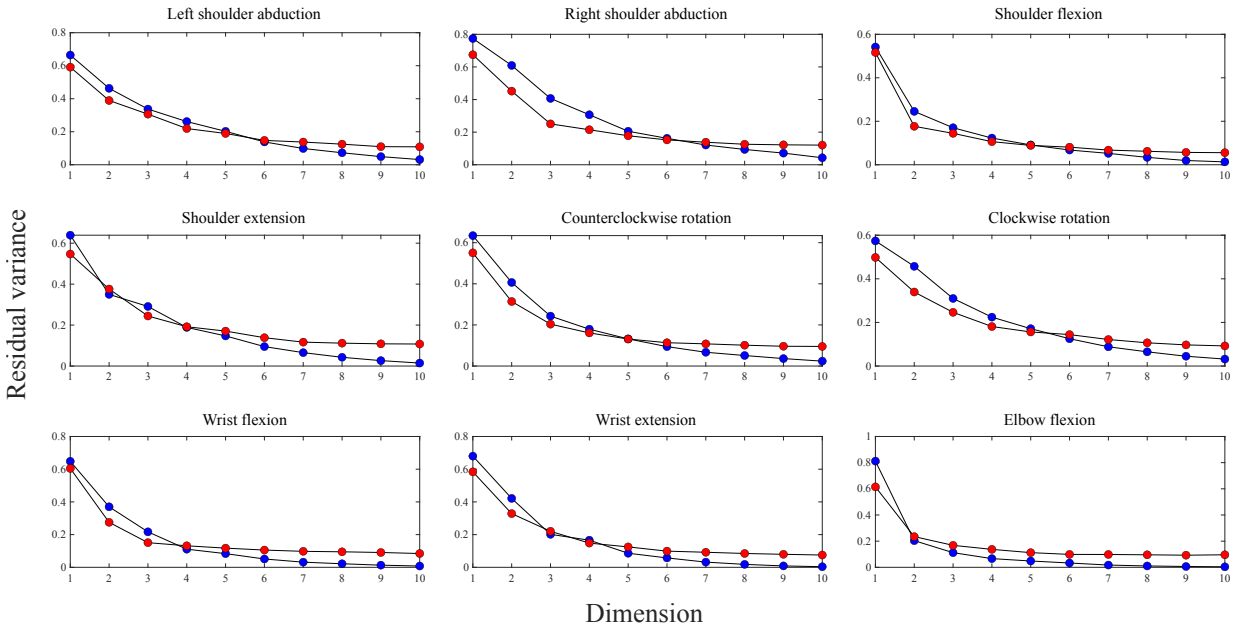

Figure 4. Residual variance of each movement for PCA (blue) and isomap (red).

Several factors might limit our findings. First, it is possible that insufficient data points were used in this study. Collecting data on more iterations of each movements might yield a more defined manifold. Second, it is tenable that noise from the Microsoft Kinect falsely led to greater variation along certain dimensions. For example, when joints are occluded from its view, the Microsoft Kinect estimates their position and introduces error into the measurement.[17] With our platform, a user may hold the dowel such that the Kinect's view of the elbow and shoulder joints is occluded by the hands. In such a case, the Kinect may introduce erroneous elbow flexion and shoulder abduction angles.[17]

In the next steps, alternative dimensionality reduction methods may be explored on larger data sets. Such methods may include diffusion maps[14] and locally linear embedding.[18] Once the method of choice is selected, different classifiers may be explored as well, including decision trees,[19] support vector machine,[20] K-nearest neighbors,[21] and RUSBoost.[22] These effort will provide insight into programmed assessment of upper-limb movements and its prospects in telerehabilitation.

ACKNOWLEDGMENTS

This study was funded by the National Science Foundation under grant number CBET-1604355 and ECCS-1928614. R.B.V. was also supported by a scholarship from Mitsui-USA Foundation.

REFERENCES

[1] Langhorne, P., Bernhardt, J., and Kwakkel, G., "Stroke rehabilitation," *The Lancet* **377**(9778), 1693–1702 (2011).

[2] Cirstea, M. C. and Levin, M. F., "Compensatory strategies for reaching in stroke," *Brain* **123**(5), 940–953 (2000).

[3] Lum, S., Lehman, S. L., and Reinkensmeyer, D. J., "The bimanual lifting rehabilitator: an adaptive machine for therapy of stroke patients," *IEEE Transactions on Rehabilitation Engineering* **3**(2), 166–174 (1995).

[4] Pink, M., "Contralateral effects of upper extremity proprioceptive neuromuscular facilitation patterns," *Physical Therapy* **61**(8), 1158–1162 (1981).

[5] Mills, V. M. and Quintana, L., "Electromyography results of exercise overflow in hemiplegic patients," *Physical Therapy* **65**(7), 1041–1045 (1985).

[6] Barak-Ventura, R., Ruiz-Marín, M., Nov, O., Raghavan, P., and Porfiri, M., "A low-cost telerehabilitation paradigm for bimanual training," *IEEE Transactions in Mechatronics* **submitted** (2020).

[7] Laut, J., Cappa, F., Nov, O., and Porfiri, M., "Increasing patient engagement in rehabilitation exercises using computer-based citizen science," *PLoS One* **10**(3), e0117013 (2015).

[8] Laut, J., Porfiri, M., and Raghavan, P., "The present and future of robotic technology in rehabilitation," *Current Physical Medicine and Rehabilitation Reports* **4**(4), 312–319 (2016).

[9] Laut, J., Henry, E., Nov, O., and Porfiri, M., "Development of a mechatronics-based citizen science platform for aquatic environmental monitoring," *IEEE/ASME Transactions on Mechatronics* **19**(5), 1541–1551 (2013).

[10] Barak-Ventura, R., Nakayama, S., Raghavan, P., Nov, O., and Porfiri, M., "The role of social interactions in motor performance: feasibility study toward enhanced motivation in telerehabilitation," *Journal of Medical Internet Research* **21**(5), e12708 (2019).

[11] Flash, T. and Hochner, B., "Motor primitives in vertebrates and invertebrates," *Current Opinion in Neurobiology* **15**(6), 660–666 (2005).

[12] Mussa-Ivaldi, F. A. and Bizzi, E., "Motor learning through the combination of primitives," *Philosophical Transactions of the Royal Society Series B: Biological Sciences* **355**(1404), 1755–1769 (2000).

[13] Tenenbaum, J. B., De Silva, V., and Langford, J. C., "A global geometric framework for nonlinear dimensionality reduction," *Science* **290**(5500), 2319–2323 (2000).

[14] Coifman, R. R., Lafon, S., Lee, A. B., Maggioni, M., Nadler, B., Warner, F., and Zucker, S. W., "Geometric diffusions as a tool for harmonic analysis and structure definition of data: Diffusion maps," *Proceedings of the National Academy of Sciences* **102**(21), 7426–7431 (2005).

[15] Jolliffe, I. T. and Cadima, J., "Principal component analysis: a review and recent developments," *Philosophical Transactions of the Royal Society A* **374**(2065), 20150202 (2016).

[16] Palermo, E., Laut, J., Nov, O., Cappa, P., and Porfiri, M., "A natural user interface to integrate citizen science and physical exercise," *PLoS ONE* **12**(2), e0172587 (2017).

[17] Huber, M., Seitz, A. L., Leeser, M., and Sternad, D., "Validity and reliability of kinect skeleton for measuring shoulder joint angles: A feasibility study," *Physiotherapy* **101**(4), 389–393 (2015).

[18] Roweis, S. T. and Saul, L. K., "Nonlinear dimensionality reduction by locally linear embedding," *Science* **290**(5500), 2323–2326 (2000).

[19] Quinlan, J. R., "Induction of decision trees," *Machine Learning* **1**(1), 81–106 (1986).

[20] Noble, W. S., "What is a support vector machine?," *Nature Biotechnology* **24**(12), 1565–1567 (2006).

[21] Sun, S. and Zhang, C., "Subspace ensembles for classification," *Physica A: Statistical Mechanics and its Applications* **385**(1), 199–207 (2007).

[22] Seiffert, C., Khoshgoftaar, T. M., Van Hulse, J., and Napolitano, A., "Rusboost: A hybrid approach to alleviating class imbalance," *IEEE Transactions on Systems, Man, and Cybernetics-Part A: Systems and Humans* **40**(1), 185–197 (2009).